School of Mathematical, Physical
and Computational Sciences

University of Reading

Department of Mathematics and Statistics

Preprint MPCS-2018-07

5 October 2018

A two-phase moving mesh finite element model of segregated competition-diffusion

by

A.R. Watkins and **M.J. Baines**

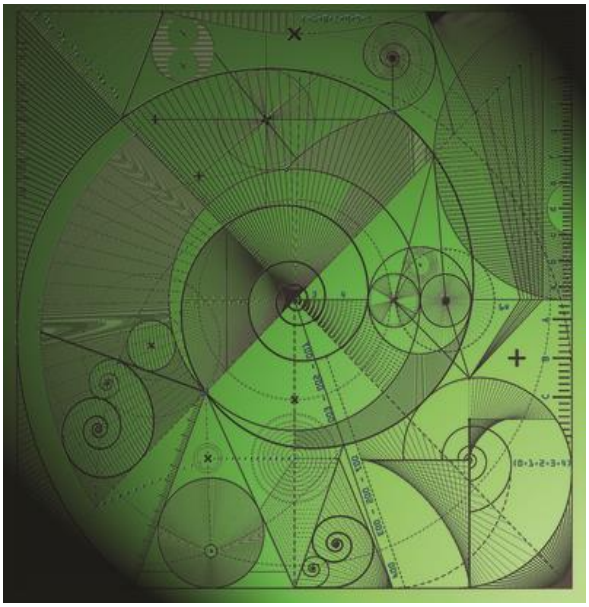

A two-phase moving mesh finite element model of segregated competition-diffusion

A. R. Watkins and M. J. Baines

Department of Mathematics and Statistics, University of Reading,
P.O.Box 220, Reading, RG6 6AX, UK

Abstract

A finite element numerical solution of the Lotka-Volterra competition-diffusion model of theoretical ecology is presented which depends on a conservation-based moving mesh. The model parameters are chosen such that the competition is strong enough to spatially segregate the two populations, leading to a two-phase problem with a coupling condition at the moving interface. Incorporation of the moving interface into the finite element solution preserves the identities of the two species in space and time, enabling parameters to be referred to each separate population as the interface moves.

1 Introduction

We consider the application of a conservation-based moving mesh finite element method [1, 3] to a model of population dynamics. A version of the Lotka-Volterra competition model is taken that describes a two-phase segregated reaction-diffusion system and the moving mesh method implemented for this system. We examine a two-phase Lotka-Volterra competition-diffusion system with a high competition limit, so that the species are completely spatially segregated and interact only though their interface using an interface condition based on this high competition limit [4, 6].

The model is implemented numerically with a variety of creative parameter combinations, and various behaviours are observed which dominate in turn as the populations evolve through time.

It is shown in [4] that where competition is strong enough to spatially segregate two populations the Lotka-Volterra PDE system can be reduced to a form similar to a Stefan problem, The Stefan problem has been considered numerically in [2] usiing a moving mesh finite element method based on conservation (MMFEM). The two major differences between the Stefan model and the Lotka-Volterra model are, firstly, there are additional logistic growth terms in the Lotka-Volterra model, and secondly, there is a parameter in the Lotka-Volterra model of the interface (the equivalent of the latent heat coefficient of the Stefan problem) which is set equal to zero. In biological terms, one species does not transform into another, which means that unlike the Stefan problem the competition system has an interface condition that does not specify an interface velocity. This presents a challenge when attempting to apply the same approach to the Lotka-Volterra model as to the Stefan problem in [2] because that paper uses the interface velocity taken directly from that condition.

However, the moving mesh finite element method approach in [2] is a promising way to model the competition system because it not only directly tracks the evolution of the interface between species, it provides a framework for keeping particular mesh nodes attached to particular species. This means that the internal dynamics of a species can be assigned to particular nodes or elements rather than particular parts of space, and the dynamics for any given location will automatically be those of the correct species.

In this paper we model, in one dimension, the system described by Hilhorst *et al.* [4] using a moving mesh finite element method (MMFEM) developed from that in [2]. We demonstrate that the MMFEM method can be extended to include logistic growth terms and also applied to problems without an explicit formula for the interface velocity.

2 The Lotka-Volterra system

The Lotka-Volterra system studied is the two-component reaction-diffusion system

$$\frac{\partial u_1}{\partial t} = \delta_1 \frac{\partial^2 u_1}{\partial x^2} + f(u_1, u_2)u_1 \qquad x \in R_1(t), \quad t > 0 \qquad (1)$$

$$\frac{\partial u_2}{\partial t} = \delta_2 \frac{\partial^2 u_2}{\partial x^2} + g(u_1, u_2)u_2 \qquad x \in R_2(t) \quad t > 0 \qquad (2)$$

where δ_1, δ_2 are constant diffusion coefficients and with (in general)

$$f(u_1, u_2) = r_1 \left(1 - \frac{u_1 + K_1 u_2}{k_1}\right)$$

$$g(u_1, u_2) = r_2 \left(1 - \frac{u_2 + K_2 u_1}{k_2}\right).$$

Here $u_1(x,t)$ and $u_2(x,t)$ are the positive population densities of two competing species in adjacent regions $R_1(t)$ and $R_2(t)$, the k_1, k_2 are the respective carrying capacities of the species, the K_1, K_2 are species-specific competition rates, and r_1, r_2 are reproductive rate parameters.

In [4] it is demonstrated that for two species completely segregated the reaction terms can be reduced to

$$f(u_1, u_2) = r_1(1 - u_1/k_1)$$

$$g(u_1, u_2) = r_2(1 - u_2/k_2).$$

so that (1) and (2) become

$$\frac{\partial u_1}{\partial t} = \delta_1 \frac{\partial^2 u_1}{\partial x^2} + \{r_1(1 - u_1/k_1)\}u_1 \qquad x \in R_1(t), \quad t > 0 \qquad (3)$$

$$\frac{\partial u_2}{\partial t} = \delta_2 \frac{\partial^2 u_2}{\partial x^2} + \{r_2(1 - u_2/k_2)\}u_2 \qquad x \in R_2(t) \quad t > 0 \qquad (4)$$

The resulting system represents the limit in which the K_1, K_2 values are very large, i.e. the competition rate is high enough that the two species cannot coexist in space. In the region populated by species 1, $u_2 = 0$, and in the region populated by species 2, $u_1 = 0$.

2.1 Boundary and initial conditions

At the interface between the two species there is a condition that gives the relationship between their fluxes. In essence, the species both flow into the

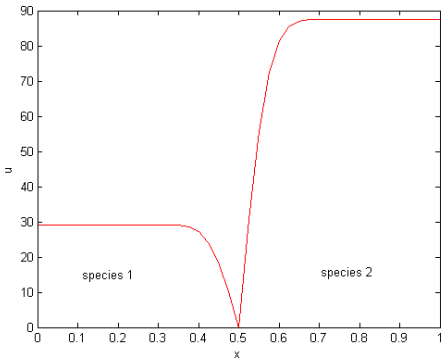

Figure 1: Initial conditions for the competition system, with population density U_1 of species 1 (on the left) and U_2 of species 2 (on the right). The interface node has zero population and must always satisfy the interface condition.

interface and annihilate each other in a ratio determined by the competition coefficient μ. This condition is given in [4] as

$$\mu\delta_1 \frac{\partial u_1}{\partial x} = -\delta_2 \frac{\partial u_2}{\partial x} \tag{5}$$

where $\mu = K_2/K_1$. We call μ the interspecies competition rate. Because the annihilation is complete we also have a zero Dirichlet condition,

$$u_1 = u_2 = 0,$$

at the interface. Zero Neumann boundary conditions $\partial u_1/\partial x = 0$ and $\partial u_2/\partial x = 0$ are applied at fixed external boundaries away from the interface.

Initial conditions on u_1 and u_2 are not given in [4], but we select suitable initial conditions and physical parameters such that one species is in growth and the other in decline. The initial conditions are shown in figure (1).

3 The MMFEM conservation method

3.1 Weak forms

We begin by writing the governing Lotka-Volterra equations (3) and (4) in the weak forms

$$\int_{R_p(t)} w(x,t)\frac{\partial u_p}{\partial t}\mathrm{d}x = \delta_p \int_{R_p(t)} w(x,t)\frac{\partial^2 u_p}{\partial x^2}\mathrm{d}x + r_p \int_{R_p(t)} w(x,t)\, u_p \left(1 - \frac{u_1}{k_1}\right)\mathrm{d}x, \tag{6}$$

$(p = 1, 2)$, where $w(x,t)$ is a positive test function.

3.2 A relative conservation principle

The total population of each species is defined as θ_p, given by

$$\theta_p(t) = \int_{R_p(t)} u_p(x,t)\,\mathrm{d}x \tag{7}$$

$(p = 1, 2)$, where $R_p(t)$ is the domain inhabited by that species.

We now introduce a relative conservation principle in each domain for each species in terms of $\theta_p(t)$ as

$$\frac{1}{\theta_p(t)} \int_{R_p(t)} w(x,t)\, u_p(x,t)\,\mathrm{d}x = c_p, \qquad (p = 1, 2), \tag{8}$$

where the population fractions c_p depend on the test function w but are otherwise independent of time. The constants c_p are determined from the initial conditions at time $t = 0$, i.e.

$$c_p = \frac{1}{\theta_p(0)} \int_{R_p(0)} w(x,0) u_p(x,0)\,\mathrm{d}x.$$

We write the relative conservation principles (8) as

$$\int_{R_p(t)} w(x,t)\, u_p(x,t)\,\mathrm{d}x = c_p\theta_p(t) = c_p \int_{R_p(t)} u_p(x,t)\,\mathrm{d}x, \qquad (p = 1, 2). \tag{9}$$

Differentiating with respect to time and using Leibnitz Integral Rule, the left hand side of (9) becomes

$$\frac{\mathrm{d}}{\mathrm{d}t}\left[\int_{R_p(t)} w(x,t)\, u_p(x,t)\mathrm{d}x\right] = \int_{R_p(t)} \left(\frac{\partial(w u_p)}{\partial t} + \frac{\partial}{\partial x}(w u_p v_p\right)\mathrm{d}x, \tag{10}$$

where $v_p(x,t)$ is the domain velocity. We suppose that the test function $w(x,t)$ moves with the velocity $v_p(x,t)$ induced by (8), so that

$$\frac{\partial w}{\partial t} + v_p \frac{\partial w}{\partial x} = 0$$

Hence (10) becomes

$$\frac{\mathrm{d}}{\mathrm{d}t}\left[\int_{R_p(t)} w(x,t)u_p(x,t)\mathrm{d}x\right] = \int_{R_p(t)} w(x,t)\frac{\partial}{\partial x}(u_p v_p \mathrm{d}x - \int_{R_p(t)} w(x,t)\frac{\partial u_p}{\partial t}\mathrm{d}x.$$

Therefore, by (9), the velocity v_p and rate of change of the total mass $\dot{\theta}_p$ in each region are given in terms of the constants c_p by

$$c_p\dot{\theta}_p - \int_{R_p(t)} w(x,t)\frac{\partial}{\partial x}(u_p\dot{x}_p)\mathrm{d}x = \int_{R_p(t)} w(x,t)\frac{\partial u_p}{\partial t}\mathrm{d}x, \qquad (p=1,2). \quad (11)$$

The boundary conditions have yet to be applied.

3.3 A velocity potentlal

At this point it is convenient to introduce a velocity potential ϕ_p, defined by

$$v_p = \frac{\partial \phi_p}{\partial x} \quad (12)$$

so that equation (11) becomes

$$c_p\dot{\theta}_p - \int_{R_p(t)} w(x,t)\frac{\partial}{\partial x}\left(u_p\frac{\partial \phi_p}{\partial x}\right)\mathrm{d}x = \int_{R_p(t)} w(x,t)\frac{\partial u_p}{\partial t}\mathrm{d}x,$$

for each species, or after integration by parts,

$$c_p\dot{\theta}_p - \left[w u_p \frac{\partial \phi_p}{\partial x}\right]_{\partial R_p(t)} + \int_{R_p(t)} u_p(x,t)\,\frac{\partial w}{\partial x}\frac{\partial \phi_p}{\partial x}\mathrm{d}x = \int_{R_p(t)} w(x,t)\frac{\partial u_p}{\partial t}\mathrm{d}x. \quad (13)$$

3.4 Substituting the Lotka-Volterra equations

We now substitute the weak form of the governing PDEs (6) into the right hand side of (13), giving after a further integration by parts,

$$\delta_p\left[w\frac{\partial u_p}{\partial x}\right]_{\partial R_p(t)} - \delta_p\int_{R_p(t)}\frac{\partial w}{\partial x}\frac{\partial u_p}{\partial x}\mathrm{d}x + r_p\int_{R_p(t)} w(x,t)u_p(x,t)\,\left(1-\frac{u_p(x,t)}{k_p}\right)\mathrm{d}x.$$

At the external boundaries $\partial u_p/\partial x = 0$ and also $v_p = \partial\phi/\partial x = 0$ because the boundaries are fixed. Together with the condition that $u_p = 0$ on the interface boundary, equation (13) for the velocity potential ϕ_p and the rate of change of the total mass $\dot{\theta}_p$ for species p becomes

$$c_p\dot{\theta}_p + \int_{R_p(t)} u_p(x,t)\,\frac{\partial w}{\partial x}\frac{\partial \phi_p}{\partial x}\mathrm{d}x = (-1)^p\delta_p\left(w\frac{\partial u_p}{\partial x}\right)\Big|_{x_m(t)} - \delta_p\int_{R_p(t)}\frac{\partial w}{\partial x}\frac{\partial u_p}{\partial x}\mathrm{d}x + r_p\int_{R_p(t)} w(x,t)u_p(x,t)\left(1-\frac{u_p(x,t)}{k_p}\right)\mathrm{d}x \tag{14}$$

$(p = 1, 2)$, where $x_m(t)$ is the interface.

Given the constants c_p, equation (14) is solved for the velocity potential ϕ_p and the rate of change of the total mass $\dot{\theta}_p$ for each species, and the velocities derived from (12).

In particular, for a test function w equal to unity, so that $c_p = 1$ from (7), equation (14) reduces to

$$\dot{\theta}_p = (-1)^p\delta_p\left(\frac{\partial u_p}{\partial x}\right)\Big|_{x_m(t)} + r_p\int_{R_p(t)} u_p(x,t)\left(1-\frac{u_p(x,t)}{k_p}\right)\mathrm{d}x \tag{15}$$

which determines $\dot{\theta}_p$.

We now consider the interface motion.

3.5 The interface condition

If this problem were a standard Stefan problem we would, as in [2], use the Stefan condition at the interface in the form

$$k_S\frac{\partial u_1}{\partial x} - k_L\frac{\partial u_2}{\partial x} = \lambda v_m$$

(where k_S, k_L, λ are given parameters and v_m is the interface velocity) to determine v_m in terms of u_1 and u_2. In contrast, the interface condition (5) for the competition system is

$$\mu\delta_1\frac{\partial u_1}{\partial x} = -\delta_2\frac{\partial u_2}{\partial x},$$

equivalent to the Stefan condition with $\lambda = 0$, not containing the velocity v_m.

Moreover, the Stefan condition refers to a situation where the gradients of u either side of the interface are of the same sign in general. In contrast, equation (5) refers to an interface where the gradients either side are of opposite polarity, since $u = 0$ on the interface and the method requires positive populations, i.e. we have interfaces with 'V' shaped functions.

Whilst the interface velocity is not given explicitly by (5) the expression does contain information about the location of the interface implicitly. Thus, if we know $\partial u/\partial x$ in the interior of each region adjacent to the interface, we may use the fact that $u = 0$ at the interface to infer an interface position. We therefore seek an interface position such that the values of $\partial u/\partial x$ either side of the interface are in the ratio $-\mu$.

3.5.1 Approximating the interface condition

We shall adopt an explicit time-stepping approach which allows us to update the species and the interface simultaneously, but only to first order in time and subject to stability limitations on the time step. Should there be a problem in this regard, a suitable alternative would be to use an implicit time integration scheme, which would accord the ability to reassign the interface position.

At any given time t we approximate the interface condition (5) in the finite difference form

$$\mu\delta_1 \frac{u_{1,m} - u_{1,m-1}}{x_m - x_{m-1}} = -\delta_2 \frac{u_{2,m+1} - u_{2,m}}{x_{m+1} - x_m},$$

where the subscript m denotes the interface node and the $x_i, u_{p,i}$, $(i = m-1, m, m+1), (p = 1, 2)$, are adjacent node positions and solution values. Since $u_m = 0$ we obtain an expression for the position of the interface node x_m in terms of adjacent nodal values at $m \pm 1$ as

$$x_m = \left(\frac{\mu\delta_1 u_{1,m-1} x_{m+1} + \delta_2 u_{2,m+1} x_{m-1}}{\mu\delta_1 u_{1,m-1} + \delta_2 u_{2,m+1}} \right). \tag{16}$$

In order to align the interface movement with the velocity-based description in (14) it is appropriate to calculate a velocity which can be used alongside the nodal velocities. This grants more flexibility in the chosen time integration scheme. We therefore construct from (16) an approximate velocity

$$\dot{x}_m = \frac{x_m - x_m^n}{\Delta t} = \frac{\left(\frac{(\mu\delta_1 u_{1,m-1}^n x_{m+1}^n + \delta_2 u_{2,m+1}^n x_{m-1}^n)}{(\mu\delta_1 u_{1,m-1}^n + \delta_2 u_{2,m+1}^n)} - x_m^n \right)}{\Delta t}. \tag{17}$$

where Δt is the time step.

3.6 Finite elements and modified basis functions

We now consider spatial approximation of the velocities of the species in the two phases. Let the regions $R_1(t) = [0, x_m(t)]$ and $R_2(t) = [x_m(t), 1]$, where $x_m(t)$ is the position of the interface. Define the mesh

$$0 = X_0 < X_1(t) < \ldots < X_m(t) < \ldots < X_N(t) < X_{N+1} = 1$$

and choose the test function $w(x,t)$ to be a member of the set $\{W\}$ of standard piecewise-linear positive basis functions W_i $(0 < i < N+1)$ appropriate to Neumann boundary conditions, except for W_{m-1}, W_m, W_{m+1}. With the known value of the population at the interface node $X_m(t)$ in mind we discard the test function W_m and augment the adjacent test functions W_{m-1}, W_{m+1} by those parts of W_m lying in the relevant phase. The resulting set of test functions, $\{\tilde{W}_i\}$ say, called modified test functions in [5, 6], form a partition of unity in each phase.

The population densities u_p in each phase are now approximated by piecewise-linear functions U_p, $(p = 1, 2)$, projections of u_p into the spaces spanned by the $\{\tilde{W}_i\}$.

The total populations in the two phases are then

$$\Theta_1(t) = \int_0^{X_m(t)} U(x,t)\,\mathrm{d}x, \qquad \Theta_2(t) = \int_{X_m(t)}^1 U(x,t)\,\mathrm{d}x \tag{18}$$

and the relative conservation principles in the two phases are

$$\frac{1}{\Theta_1(t)} \int_0^{X_m(t)} W_i\, U_1(x,t)\,\mathrm{d}x = c_{1,i}, \qquad \frac{1}{\Theta_2(t)} \int_{X_m(t)}^1 W_i\, U_2(x,t)\,\mathrm{d}x = c_{2,i}.$$

where the constant-in-time partial populations $c_{1,i}$ and $c_{2,i}$ are obtained from (8) and the initial conditions at $t = 0$, giving

$$c_{1,i} = \frac{1}{\Theta_1(0)} \int_0^{X_m(0)} \tilde{W}_i(x,0) U_1(x,0)\mathrm{d}x, \quad c_{2,i} = \frac{1}{\Theta_2(0)} \int_{X_m(0)}^1 \tilde{W}_i(x,0) U_2(x,0)\mathrm{d}x.$$

Note that due to the construction of the $\tilde{W}_i$ both $\sum_{i=0}^{m-1} c_{1,i}$ and $\sum_{i=m+1}^{N+1} c_{2,i}$ are equal to unity.

3.6.1 The finite element velocity potentials

We now substitute piecewise-linear finite element functions Φ_1, Φ_2 for ϕ_1, ϕ_2 into (14) to obtain, in phase 1,

$$\int_0^{X_m(t)} U_1(x,t)\,\frac{\partial \tilde{W}_i}{\partial x}\frac{\partial \Phi_1}{\partial x}\mathrm{d}x = -c_{1,i}\dot{\Theta}_1 - \delta_1 \int_0^{X_m(t)} \frac{\partial \tilde{W}_i}{\partial x}\frac{\partial U_1}{\partial x}\mathrm{d}x + \delta_1 \left(W_i \frac{\partial U_1}{\partial x}\right)\Big|_{m(t)}$$
$$+ r_1 \int_0^{X_m(t)} \tilde{W}_i(x,t) U_1(x,t)\left(1 - \frac{U_1(x,t)}{k_1}\right)\mathrm{d}x, \qquad (i = 0, \ldots, m) \qquad (19)$$

and, in phase 2,

$$\int_{X_m(t)}^1 U_2(x,t)\,\frac{\partial \tilde{W}_i}{\partial x}\frac{\partial \Phi_2}{\partial x}\mathrm{d}x = -c_{2,i}\dot{\Theta}_2 - \delta_2 \int_{X_m(t)}^1 \frac{\partial \tilde{W}_i}{\partial x}\frac{\partial U_2}{\partial x}\mathrm{d}x - \delta_2 \left(W_i \frac{\partial U_2}{\partial x}\right)\Big|_{m(t)}$$
$$+ r_2 \int_{X_m(t)}^1 \tilde{W}_i(x,t) U_2(x,t)\left(1 - \frac{U_2(x,t)}{k_2}\right)\mathrm{d}x, \qquad (i = m, \ldots, N+1). \qquad (20)$$

The final integrals in (19) and (20) may be evaluated exactly using Simpson's rule.

Since the $\tilde{W}_i$ form a partition of unity in each phase, the rates of change $\dot{\theta}_1$ and $\dot{\theta}_2$ of the populations are obtained by summing (19) and (20) over the relevant i to obtain

$$\dot{\Theta}_1 = \delta_1 \frac{\partial U_1}{\partial x}\Big|_{X_m(t)} + r_1 \int_0^{X_m(t)} U_1(x,t)\left(1 - \frac{U_1(x,t)}{k_1}\right)\mathrm{d}x \qquad (21)$$

and

$$\dot{\Theta}_2 = -\,\delta_2 \frac{\partial U_2}{\partial x}\Big|_{X_m(t)} + r_2 \int_{X_m(t)}^1 U_2(x,t)\left(1 - \frac{U_2(x,t)}{k_2}\right)\mathrm{d}x. \qquad (22)$$

We solve equations (21) and (22) for $\dot{\Theta}_1$ and $\dot{\Theta}_2$, followed by (19) and (20) for Φ_1, Φ_2, respectively, with a zero Dirichlet condition on Φ_1 or Φ_2 at the interface (which is no restriction since only the derivatives of Φ_1, Φ_2 are required for the velocities).

3.6.2 The finite element velocities

In order to derive the finite element nodal velocities $V_1(x,t), V_2(x,t)$ from Φ_1, Φ_2 we return to the definition (12) of v in terms of ϕ, now written in the

weak forms

$$\int_0^{X_m(t)} \tilde{W}_i(x,t)V_1(x,t)\,\mathrm{d}x = \int_0^{X_m(t)} \tilde{W}_i\frac{\partial \Phi_1}{\partial x}\mathrm{d}x \tag{23}$$

in phase 1, or

$$\int_{X_m(t)}^1 \tilde{W}_i(x,t)V_2(x,t)\,\mathrm{d}x = \int_{X_m(t)}^1 \tilde{W}_i\frac{\partial \Phi_2}{\partial x}\mathrm{d}x \tag{24}$$

in phase 2, and solve for V_1 and V_2, except at the interface where (17) is applied.

3.6.3 The finite element mesh

Having obtained the velocities $V_1(x,t)$ and $V_2(x,t)$, we derive piecewise-linear nodal functions $X_1(x,t), X_2(x,t)$ at the new time level using the explicit Euler time-stepping scheme with a stable time step Δt chosen to ensure stability. We also update Θ_1 and Θ_2 from (21) and (22) using the same scheme.

For the interface itself we apply the explicit Euler scheme to the interface velocity (17), resulting in

$$X_m^{n+1} = \left(\frac{\mu\,\delta_1\,U_{1,m-1}^n X_{m+1}^n + \delta_2\,U_{2,m+1}^n X_{m-1}^n}{\mu\,\delta_1\,U_{1,m-1}^n + \delta_2\,U_{2,m+1}^n}\right) \tag{25}$$

3.6.4 The finite element population densities

We now use (9) to determine the finite element population densities $U_1(x,t)$ and $U_2(x,t)$ at the new time step $t = t^{n+1}$. For species 1 we have

$$\int_0^{X_m(t)} \tilde{W}_i(x,t)\,U_1(x,t)\,\mathrm{d}x = c_{1,i}\Theta_1(t) \tag{26}$$

and for species 2,

$$\int_{X_m(t)}^1 \tilde{W}_i(x,t)U_2(x,t)\,\mathrm{d}x = c_{2,i}\Theta_2(t). \tag{27}$$

We solve (26) and (27) for the positive densities $U_1(x,t^{n+1})$ and $U_2(x,t^{n+1})$ with the zero Dirichlet condition at the interface imposed strongly.

3.7 Matrix forms

3.7.1 The velocity potentials

We expand $\Phi_1(x,t), \Phi_2(x,t)$ in terms of standard piecewise-linear basis functions $W_j(x,t)$ as

$$\Phi_1(x,t) = \sum_{j=0}^{m-1} \Phi_{1,j} W_j(x,t), \qquad \Phi_2(x,t) = \sum_{j=m+1}^{N+1} \Phi_{2,j} W_j(x,t)$$

These forms may be substituted into (19) and (20), where $\dot{\Theta}_1$ is given by (21) and $\dot{\Theta}_2$ by (22), and the resulting systems written in matrix form.

Equations (19) and (20) can then be expressed in the form

$$\tilde{K}(\underline{U}_1)\ \underline{\Phi}_1 = \underline{\tilde{f}}_1 \qquad \tilde{K}(\underline{U}_2)\ \underline{\Phi}_2 = \underline{\tilde{f}}_2 \tag{28}$$

where $\tilde{K}(\underline{U}_1)$, $\tilde{K}(\underline{U}_2)$ are weighted stiffness matrices constructed with the modified basis functions $\tilde{W}_i$, having entries

$$\int_0^{X_m(t)} U_1(x,t)(\tilde{W}_i)_x\,(W_j)_x\,\mathrm{d}x, \qquad (i,j = 0,\ldots,m-1),$$

and

$$\int_{X_m(t)}^1 U_2(x,t)(\tilde{W}_i)_x\,(W_j)_x\,\mathrm{d}x, \qquad (i,j = m+1,\ldots,N+1).$$

The vector $\underline{\Phi}_p$ contains the coefficients $\Phi_{p,j}$, $(p = 1,2)$, and $\underline{\tilde{f}}_p$, $\underline{\tilde{f}}_p$, are vectors whose entries are the right hand sides of (19),(20), respectively.

Since the matrices $\tilde{K}(\underline{U}_1)$ and $\tilde{K}(\underline{U}_2)$ are both singular (the rows of the left hand sides of both (19) and (20) sum to zero), each of the systems (28) have an infinity of solutions. We set $\Phi_{p,m} = 0$ at the interface node to obtain unique solutions for $\Phi_1(x,t)$ and $\Phi_2(x,t)$. (The rates of change $\dot{\Theta}_1$ and $\dot{\Theta}_2$ can be found in a straightforward manner by simply summing the rows of equations (28).)

3.7.2 The velocities

In order to derive the velocities we use the expansions

$$V_1(x,t) = \sum_{j=0}^{m-1} V_{1,j}(t) W_j(x,t), \qquad V_2(x,t) = \sum_{j=m+1}^{N+1} V_{2,j}(t) W_j(x,t)$$

substituted into equation (23) and (24) to obtain

$$\sum_{j=0}^{m-1}\left[\int_0^{X_m(t)}\tilde{W}_i W_j \mathrm{d}x\right] V_{1,j} = \sum_{j=0}^{m-1}\left[\int_0^{X_m(t)}\tilde{W}_i \frac{\partial W_j}{\partial x}\mathrm{d}x\right]\Phi_{1,j} \qquad (29)$$

and

$$\sum_{j=m+1}^{N+1}\left[\int_{X_m(t)}^{1}\tilde{W}_i W_j \mathrm{d}x\right] V_{2,j} = \sum_{j=m+1}^{N+1}\left[\int_{X_m(t)}^{1}\tilde{W}_i \frac{\partial W_j}{\partial x}\mathrm{d}x\right]\Phi_{2,j} \qquad (30)$$

In matrix form equations (29) and (30) can be written

$$\tilde{M}_1\underline{V}_1 = \tilde{B}_1\underline{\Phi}_1 \qquad \tilde{M}_2\underline{V}_2 = \tilde{B}_2\underline{\Phi}_2. \qquad (31)$$

where $\tilde{M}_1$, $\tilde{B}_1$ are matrices with entries

$$\int_0^{X_m(t)}\tilde{W}_i\, W_j\,\mathrm{d}x, \quad \int_0^{X_m(t)}\tilde{W}_i\,(W_x)_j\,\mathrm{d}x, \qquad (i,j=1,\ldots,m-1) \qquad (32)$$

and the vectors $\underline{V}_1$, $\underline{\Phi}_1$ contain the values of $V_{1,j}$, $\Phi_{1,j}, (j=1,\ldots,m-1)$. Similarly, $\tilde{M}_2$, $\tilde{B}_2$ have entries

$$\int_{X_m(t)}^{1}\tilde{W}_i\, W_j\,\mathrm{d}x, \quad \int_{X_m(t)}^{1}\tilde{W}_i\,(W_x)_j\,\mathrm{d}x, \qquad (i,j=m+1,\ldots,N+1), \quad (33)$$

and $\underline{V}_{2,j}$, $\underline{\Phi}_2$ contain the values of $V_{2,j}$, $\Phi_{2,j}, (j=m+1,\ldots,N+1)$.

The explicit Euler scheme is applied to $V_{p,j}(t)$, $\dot{\Theta}_p(t)$, $(p=1,2)$, as well as X_m (using (17)) to give all the $X_{p,j}$ and the Θ_p.

3.7.3 The population densities

Once the nodes $X_{p,j}$ and the Θ_p have been found at the new time level, $U_1(x,t)$ and $U_2(x,t)$ are determined on the updated grid from (8).

Expanding $U_1(x,t), U_2(x,t)$ in terms of standard piecewise-linear basis functions $W_j(x,t)$ (as are appropriate to Neumann conditions at external boundaries),

$$U_1(x,t) = \sum_{j=0}^{m-1} U_{1,j}(t)W_j(x,t), \qquad U_2(x,t) = \sum_{j=m+1}^{N+1} U_{2,j}(t)W_j(x,t)$$

equations (8) become

$$\frac{1}{\Theta_1(t)}\int_0^{X_m(t)} \tilde{W}_i \sum_{j=0}^{m-1} U_{1,j}(t) W_j(x,t)\,\mathrm{d}x = \tilde{C}_{1,i},$$

and

$$\frac{1}{\Theta_2(t)}\int_{X_m(t)}^{1} \tilde{W}_i \sum_{j=m+1}^{N+1} U_{2,j}(t) W_j(x,t)\,\mathrm{d}x = \tilde{C}_{2,i},$$

say. In matrix form these are

$$\tilde{M}_1 \underline{U}_1 = \underline{\tilde{C}}_1 \Theta_1(t) \quad \text{and} \quad \tilde{M}_2 \underline{U}_2 = \underline{\tilde{C}}_2 \Theta_2(t), \tag{34}$$

where $\tilde{M}_1$, $\tilde{M}_2$ are matrices with entries given by the first of (32) and the first of (33), $\underline{U}_p$, $(p = 1, 2)$, are vectors containing the $U_{p,j}$, and $\underline{\tilde{C}}_1, \underline{\tilde{C}}_2$ are vectors with entries $\tilde{C}_{1,i}$, $(i = 0, \ldots, m-1)$, $\tilde{C}_{2,i}$, $(i = m+1, \ldots, 1)$, respectively.

To find the constants $\underline{\tilde{C}}_{1,i}$ and $\underline{\tilde{C}}_{2,i}$ we set $t = 0$ and use the initial conditions in (34). For each subsequent time step we calculate the mass matrices $\tilde{M}_1$ and $\tilde{M}_2$ on the updated grid. We can then obtain the updated $\underline{U}_1$ and $\underline{U}_2$ from (34).

In summary, the conservation-based moving mesh finite element solution of the competition problem given by equations (3) and (4) with an interface condition given by (5) consists of the following steps.

3.8 Algorithm

From the initial data and the initial mesh compute

1. the projections U_p of u_p, $(p = 1, 2)$,
2. the values of the relative masses $\tilde{C}_{1_i}$ and $\tilde{C}_{2_i}$ from (34), and
3. the initial values of the total populations $\Theta_1(0)$ and $\Theta_2(0)$ from (18).

Then at each time step:

1. Find the velocity potentials $\Phi_1(t)$ and $\Phi_2(t)$by solving equations (28),
2. Find the interior nodal velocities $\underline{V}_1(t)$ and $\underline{V}_2(t)$ by solving equations (31),

3. Find the position of the interface node X_m at the next time step from (25) and estimate the interface velocity,

4. Generate the nodal positions $X_{i,j}$, $X_{2,j}$ at the next time-step from $V_{1,j}$, $V_{2,j}$ and the interface velocity, using the explicit Euler scheme,

5. Update the values of Θ_1 and Θ_2 from $\dot{\Theta}_1$ and $\dot{\Theta}_2$ using the same Euler scheme,

6. Find the population densities $\underline{U}_1$ and $\underline{U}_2$ at the next time level by solving equations (34).

4 Results

There is a vast range of parameter values in use because there are so many varied but suitable examples of the type of competition. We select a conservatively representative set of parameters, chosen to demonstrate some of the behaviours that this model is able to describe.

4.1 A parameter choice

Firstly we choose a set of parameters that favour species 1, as shown in figure 2. In this case we see an increasing interface velocity in the initial stages, followed by a long steady phase where the interface velocity is approximately constant (figure 3). As we approach the annihilation of species 2, the interface velocity increases again (figure 4). This is due to the low population of species 2 affecting its ability to grow. The movement of the interface is shown in figure 5.

4.2 Alternative parameter choices

4.2.1 Carrying capacities

We now investigate other parameter choices. We restrict the growth of species 1 by lowering its carrying capacity k_1. We observe that in this scenario neither species is dominant, even though all the competition and diffusion characteristics are unchanged. This scenario is shown in figure 6.

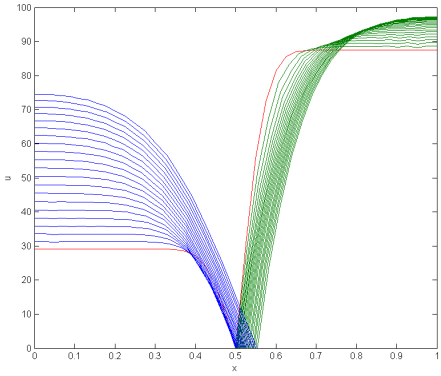

Figure 2: Result of competition model at $t = 1.7$. Here we use $\delta_1 = \delta_2 = 0.01$, $k_1 = k_2 = 100$, $r_1 = r_2 = 1$ and $\mu 3$. We run the model with a time step of 0.0001 for 17000 steps and plot the results every 0.1. We see the internal dynamics of the species driving the population densities and interface fluxes, and the position of the interface responding to those fluxes. The initial conditions are shown in red, with species 1 in blue and species 2 in green.

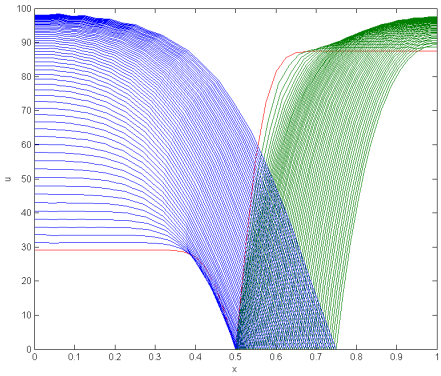

Figure 3: Result of competition model at $t = 6.0$. Here we use $\delta_1 = \delta_2 = 0.01$, $k_1 = k_2 = 100$, $r_1 = r_2 = 1$ and $\mu = 3$. We run the model with a time step of 0.0001 for 60000 steps and plot the results every 0.1. The interface continues to evolve and the populations of the species are now limited by the respective carrying capacities. The initial conditions are shown in red, with species 1 in blue and species 2 in green

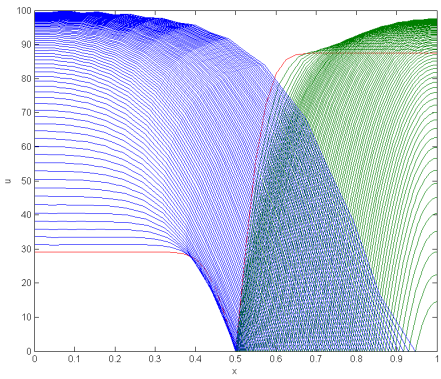

Figure 4: Result of competition model at $t = 8.8$. Here we use $\delta_1 = \delta_2 = 0.01$, $k_1 = k_2 = 100$, $r_1 = r_2 = 1$ and $\mu = 3$. We run the model with a time step of 0.0001 for 88000 steps and plot the results every 0.1. We observe that whilst the population of species 2 initially grew, it will now be wiped out by competition with species 1.

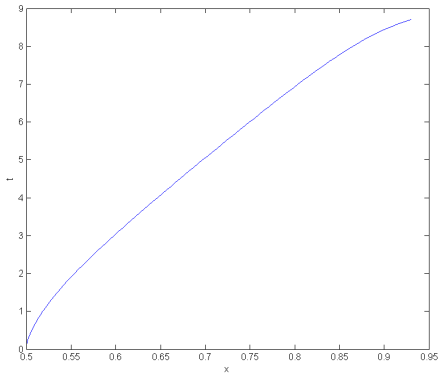

Figure 5: Movement of interface position x_m for competition model with parameters $\delta_1 = \delta_2 = 0.01$, $k_1 = k_2 = 100$, $r_1 = r_2 = 1$ and $\mu = 3$. We run the model with a time step of 0.0001. We see the interface increase in velocity after a slower initial phase where both species are experiencing population growth. We see the interface velocity accelerate as we approach an annihilation event.

4.2.2 Diffusion characteristics

Alternatively, we may adjust the diffusion characteristics of the system. By allowing species 2 to diffuse at a higher rate, we observe that species 2 is able

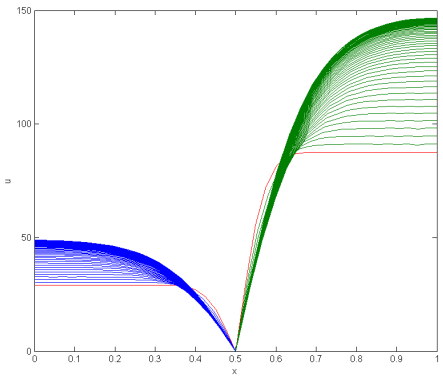

Figure 6: Result of competition model at $t = 8$, considering the effect of altered carrying capacities. Here we use $\delta_1 = \delta_2 = 0.01$, $k_1 = 50, k_2 = 150$, $r_1 = r_2 = 1$ and $\lambda = 3$. We run the model with a time step of 0.0001 for 80000 steps and plot the results every 0.1. We see that with differently chosen carrying capacities we find the interface position is approximately steady and these two species are in balance.

to make territorial gains due to this property alone (figure 7). However, as time goes on, the growth and competition characteristics become increasingly important. We see species 1 becoming more dominant over time, so that the interface velocity actually reverses direction. Figure 8 shows the evolution of the system at $t = 12.3$, and figure 9 shows the movement of the interface with the direction reversal.

These results give confidence that this model is likely to be able to satisfy the requirements of modelling a wide variety of competition systems. It is stable to a large choice of set-up parameters and is able to produce complex behaviours without problems.

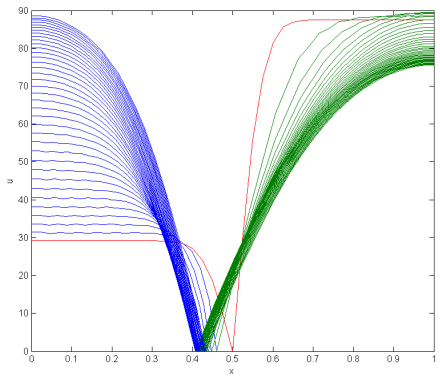

Figure 7: Result of competition model at $t = 3.5$, considering the effect of an increased diffusion rate for species 2. Here we use $\delta_1 = 0.01, \delta_2 = 0.05$, $k_1 = k_2 = 100$, $r_1 = r_2 = 1$ and $\mu = 3$. We run the model with a time step of 0.0001 for 35000 steps, and plot the results every 0.1. We observe that species 2 is able to make initial territorial gains due to its high diffusion rate, even though the competition rate is unaltered.

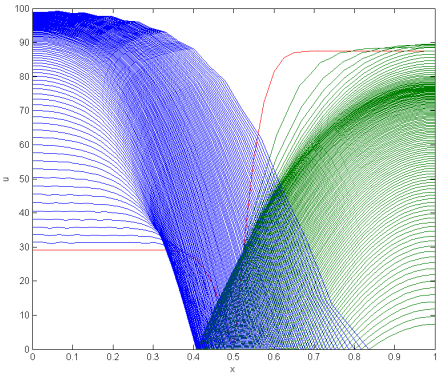

Figure 8: Result of competition model at $t = 12.3$, considering the effect of an increased diffusion rate for species 2. Here we use $\delta_1 = 0.01, \delta_2 = 0.05$, $k_1 = k_2 = 100$, $r_1 = r_2 = 1$ and $\mu = 3$. We run the model with a time step of 0.0001 for 123000 iterations, and plot the results every 0.1. We see that the initial diffusion-driven gains by species 2 are reversed, and that the overall growth characteristics are dominating so that species 1 is gaining territory.

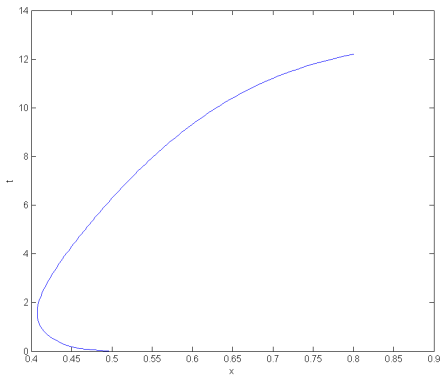

Figure 9: Position of interface, x_m, showing interface movement for the competition model at up to $t = 12.3$, considering the effect of an increased diffusion rate for species 2 (*cf.* figure 5). Here we use $\delta_1 = 0.01, \delta_2 = 0.05$, $k_1 = k_2 = 100$, $r_1 = r_2 = 1$ and $\mu = 3$. We run the model with a time step of 0.0001 for 123000 iterations, and plot the results every 0.1. Due to the growth characteristics we can see interesting temporal effects. Here the interface velocity has actually reversed direction as the system changes from diffusion-dominated to growth-dominated.

5 Summary

In this paper we have applied a moving mesh finite element method based on the relative conservation principle (MMFEM) of [2] to a two-phase Lotka-Volterra competition system with a high competition limit [4], so that the species are completely spatially segregated and interact solely through an interface condition based on this limit.

The model and the MMFEM method are described in detail and the approach implemented for a variety of parameter combinations, observing the various behaviours that dominate as the species evolve through time.

For a set of parameters that favour species 1 we see an increasing interface velocity in the initial stages followed by a long steady phase where the interface velocity is approximately constant. Although the population of species 2 initially grows it is eventually wiped out by the competition with species 1. As the annihilation of species 2 is approached, the interface velocity increases again. The interface continues to evolve and the populations of the species are then limited by the respective carrying capacities. This is due to the low

population of species 2 affecting its ability to grow.

If the growth of species 1 is restricted by lowering its carrying capacity we observe that neither species is dominant, even though all the competition and diffusion characteristics are unchanged. Increasing the diffusion rate for species 2, this species is able to make initial territorial gains, even though the competition rate is unaltered. However, as time goes on, growth and competition characteristics become increasingly important so that species 1 becomes more dominant and the interface velocity reverses direction.

A natural extension is to two dimensions along the lines described in [2]: a first attempt appears in reference [6] which foundered only on stability issues. In further work it would be interesting to compare the behaviour of the model against an empirical data set. The model easily lends itself to alterations to the logistic terms and of course changes to parameters without the need for any further development. This research would focus on collaboration in order to understand the particular modelling requirements of real-world systems which can be described in a similar manner to this model. The aim should be to understand the requirements from both a mathematical and quantitative perspective.

References

[1] M.J. Baines, M.E. Hubbard, and P.K. Jimack, *A Moving Mesh Finite Element Algorithm for the Adaptive Solution of Time-Dependent Partial Differential Equations with Moving Boundaries*, Appl. Numer. Math., 54, pp. 450-469, 2005).

[2] M.J. Baines, M.E. Hubbard, P.K. Jimack, and R. Mahmoud, A moving-mesh finite element method and its application to the numerical solution of phase-change problems), Commun in Comput.Phys., 6. pp. 595-624 (2009).

[3] M.J. Baines, M.E. Hubbard, and P.K. Jimack, *Velocity-based moving mesh methods for nonlinear partial differential equations*, Commun. Comput. Phys., 10, pp. 509-576, 2011.

[4] Hilhorst, D and Mimura, M and Schätzle, R *Vanishing latent heat limit in a Stefan-like problem arising in biology*, Nonlinear analysis: real world applications, 4, pp.261-285, 2003.

[5] M.E.Hubbard, M.J.Baines, and P.K.Jimack, *Mass-conserving Dirichlet boundary conditions for a moving-mesh finite element algorithm*, Appl. Numer. Math., 59, pp.1337-1353 (2009).

[6] A.R.Watkins, *A Moving Mesh Finite Element Method and its Application to Population Dynamics*, PhD thesis, University of Reading, UK (2017),